Journal of Thermal Analysis and Calorimetry, Vol. 80 (2005) 503–509

THERMAL BEHAVIOR OF Fe_2O_3/TiO_2 MESOPOROUS GELS

V. Balek[1*], *N. Todorova*[2], *C. Trapalis*[2], *V. Štengl*[3], *E.Večerníková*[3], *J. Šubrt*[3], *Z. Malek*[1] *and G. Kordas*[2]

[1]Nuclear Research Institute Řež, plc, 250 68 Řež, Czech Republic
[2]Institute of Materials Science, NCSR DEMOKRITOS, 15310 Athens, Greece
[3]Institute of Inorganic Chemistry, ASCR, 250 68 Řež, Czech Republic

Titania-based photocatalytic materials were prepared by sol–gel method using Fe^{3+} and polyethyleneglycol (PEG_{600}) as additives. Thermogravimetry (TG), differential thermal analysis (DTA) and evolved gas analysis (EGA) with MS detection were used to elucidate processes that take place during heating of Fe^{3+} containing titania gels. The microstructure development of the Fe_2O_3/TiO_2 gel samples with and without PEG_{600} admixtures was characterized by emanation thermal analysis (ETA) under in situ heating in air. A mathematical model was used for the evaluation of ETA results. Surface area and porosity measurements of the samples dried at 120°C and the samples preheated for 1 h to 300 and 500°C were compared. From the XRD measurements it was confirmed that the crystallization of anatase took place after thermal heating up to 600°C.

Keywords: *annealing, DTA, EGA, emanation thermal analysis, Fe_2O_3/TiO_2, porosity, sol-gel, surface area, thermogravimetry*

Introduction

TiO_2 is a photocatalyst used in wide range of environmental processes because of its unique properties: it is a semiconductor with band gap about 3.0 eV possessing strong oxidative ability and non-toxicity [1–3]. However, there are some disadvantages of its use as a photocatalyst, namely the light adsorption in UV light spectrum region only and the high electron (e^-) – hole (h^+) recombination rate. These disadvantages have been faced e.g. by doping TiO_2 with transition metal ions or by special heat treatments [4, 5]. Some of the metal ions, like Ag^+ and Fe^{3+}, when used as additives, have provoked an additional antibacterial activity of the titania photocatalyst [6–9]. It is well known that high specific surface area is a desirable property of catalytic materials. The addition of polyethylenglycol (PEG) to TiO_2 based gels was reported to increase their surface area and to improve their photocatalytic activity [10–15]. In this work, Fe^{3+} and PEG with average molecular mass 600 (PEG_{600}) were used as dopants for TiO_2 based materials to improve their properties, namely to extend the light absorption into the visible light region, to reduce the recombination of the photogenerated e^- and h^+ and to increase the surface area.

The purpose of this study is to characterize the thermal behavior of Fe_2O_3/TiO_2 gel samples and the effect of PEG_{600} admixture on their microstructure development. Methods of TG, DTA and EGA were used to elucidate processes that take place during heating of the Fe_2O_3/TiO_2 meso-porous materials. The microstructure development was characterized by emanation thermal analysis (ETA) [16, 17] under in situ heating in air. The ETA was already used in our previous studies to monitor the microstructure development of titania samples during heating of their precursors. A good agreement was found between the ETA results, surface area measurements and microstructure characteristics obtained by electron microscopy [18].

Experimental

Preparation of the samples

Sol–gel technique was used to prepare Fe^{3+} containing mesoporous titania gels with and without polyethylene glycol (PEG_{600}) addition. The amount of 76.34 mL tetrabutylorthotitanate $Ti(OBu)_4$ (Fluka) was dissolved in 245.84 mL ethanol (C_2H_5OH) absolute (Riedel–de Haen) under vigorous stirring at room temperature for 1 h. The used molar ratio was $Ti(OBu)_4$:C_2H_5OH= 0.093:2.465. The iron(III) nitrate nonahydrate (Merck) was used as the precursor for Fe^{3+} and for water in the titania based gel preparation. A solution of 13.58 mL $Fe(NO_3)_3 \cdot 9H_2O$ in 100 mL ethanol was added to the Ti containing solution and stirred for 1 h. In order to provide acidic conditions the amount of 5 mL 65% HNO_3 (Ferak) was added. The PEG_{600} containing sol (0.035 M) was prepared by

* Author for correspondence: bal@ujv.cz

1388–6150/$20.00

Akadémiai Kiadó, Budapest, Hungary
Springer, Dordrecht, The Netherlands

addition of 2.25 g PEG_{600} (Merck) under stirring for 2 h. The air dried gels that contained approximately 18 and 20 mass% of water (for sample with and without PEG_{600}, respectively) were heated at 120°C and calcined at temperatures of 300 and 500°C for 1 h.

Methods of characterization

The ETA was used in order to characterize microstructure changes of the samples under in situ conditions of heating [17]. The measurements were carried out on heating in air flow (flow rate 50 mL min^{-1}) by using Netzsch ETA-DTA equipment Model 404. The ETA is based on the measurement of the release of radon from the samples previously labeled. The sample amount was 0.1 g and alumina crucible was used. The labeling of the samples for ETA was carried out by using adsorption of ^{228}Th and ^{224}Ra radionuclides from acetone solution [16]. The specific activity of the sample was 10^5 Bq g^{-1}. The recoil depths of ^{224}Ra and ^{220}Rn ions implanted by the recoil energy (85 keV at^{-1}) into anatase were: 21 nm (straggling 6 nm), and 27 nm (straggling 6 nm), respectively as calculated by means of the TRIM code [19]. It was supposed that the maximal depth of the radon atoms penetration was 67 nm. The labeled samples were heated at the rate of 6 K min^{-1} in the air flow (flow rate 50 mL min^{-1}). The ETA results are presented as temperature dependences of the radon release rate E (in relative units): $E=A_\alpha/A_{total}$, where A_α is α-radioactivity of radon released in unit time from the labeled sample, and A_{total} is the total γ-radioactivity of the labeled sample. The A_{total} value is proportional to the rate of radon formation in the sample.

Simultaneous measurements of TG, DTA and EGA were carried out on air heating at the rate 6 K min^{-1} by Netzsch equipment Model STA 429. Alumina crucibles were used. Surface area and porosity measurements were carried out by COULTER SA 3100 equipment by using nitrogen adsorption/desorption measurements at the temperature of 77 K. The results obtained were evaluated by BET method for surface determination and by BJH method for open porosity determination, respectively.

The samples were characterized by X-ray diffraction (XRD) technique using SIEMENS D500 diffractometer with secondary graphite monochromator and CuK_α radiation. The measurements were performed by using the following combination of slits: 1.0°/1.0°1.0° as aperture diaphragms, 0.15° as detector diaphragm and 0.15° as diffracted beam monochromator diaphragm. The measured 2θ range was scanned in steps of 0.03° in 3 s/step. The size of the crystallites responsible for the Bragg reflection was determined using the Scherrer relationship [20], $d=k\lambda/(b\cos\theta)$, where d is the crystallite diameter in Å, k the shape constant (~0.9), λ the wavelength in Å, θ the Bragg angle in degrees, and b the observed peak width at half-maximum peak height in rad.

Results and discussion

Results of TG, DTA and EGA (MS detection) in Figs 1a and b demonstrated that the thermal decomposition of the Fe_2O_3/TiO_2 air dried gel samples, both without and with PEG_{600} admixture, took place on heating in the range from 50 to 400°C. The total mass loss in this temperature range determined by TG was 33 and 47%, respectively.

Two stages of the mass loss were observed, the first one that terminated at about 150°C was attributed to water release. The thermal degradation of PEG_{600} in the Fe_2O_3/TiO_2 gel sample (Fig. 1b) took place on heating from 225 to 400°C. As observed by other authors [15, 21] the thermal degradation of the free PEG_{600} macromolecules started at the temperature of 325°C; so we can suppose that the presence of metal oxides TiO_2 and Fe_2O_3 in the gel sample caused the lowering of the PEG_{600} degradation temperature.

From the ETA results in Figs 1a and b it followed that the radon release rate was enhanced by the thermal degradation of the gels, especially in the temperature range 50–250°C where the release of H_2O and CO_2 was observed by EGA (MS detection). The ETA measurements were monitoring the increase of surface area and porosity of the samples.

From Table 1 it is obvious that values of surface area and porosity of the samples both with and with-

Table 1 Surface area and porosity of Fe_2O_3/TiO_2 gel samples

Fe_2O_3/TiO_2 gel without PEG_{600}	Surface area/m^2 g^{-1}	Porosity/mL g^{-1}
heated at 120°C	11.3	0.056
heated at 300°C	245.9	0.181
heated at 500°C	75.8	0.119
Fe_2O_3/TiO_2 gel with PEG_{600}	Surface area/m^2 g^{-1}	Porosity/mL g^{-1}
heated at 120°C	1.89	0.046
heated at 300°C	350.4	0.265
heated at 500°C	42.7	0.057

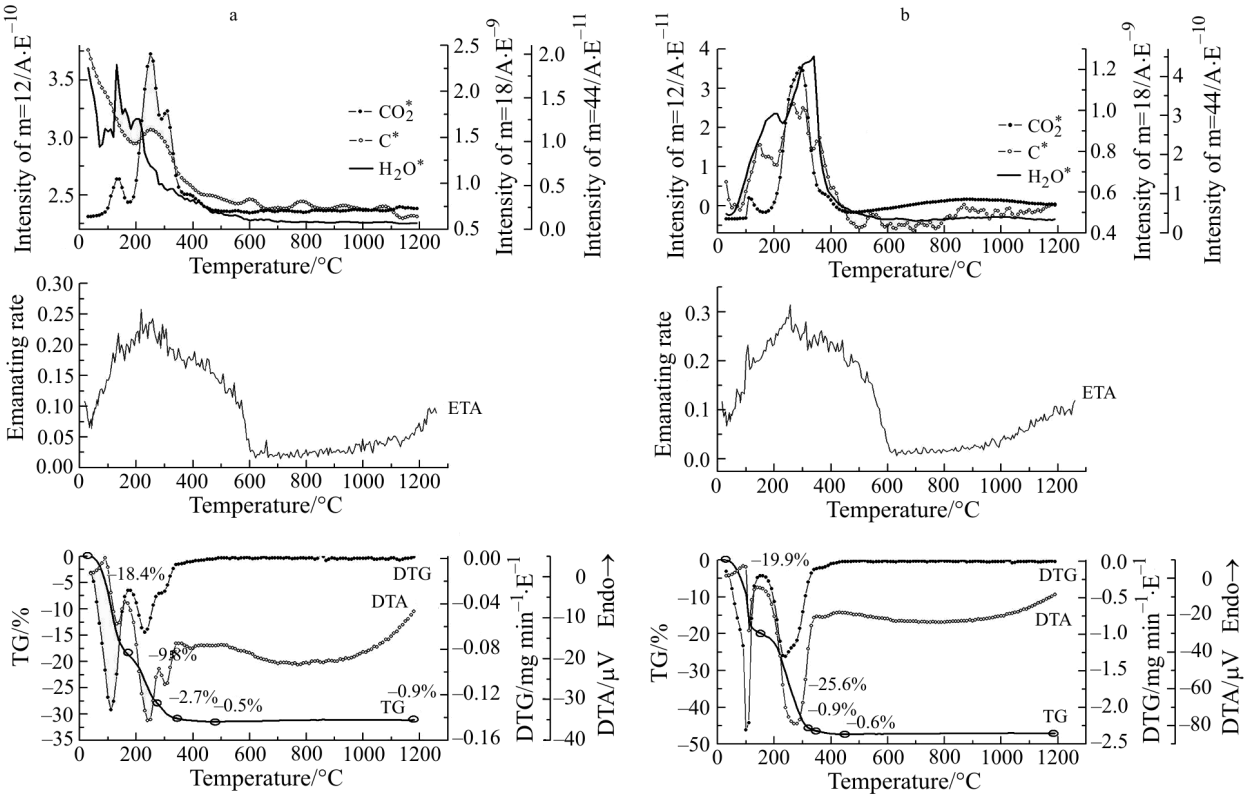

Fig. 1 TG, DTA and EGA (MS detection) results and emanation thermal analysis results of the Fe_2O_3/TiO_2 gel samples. Measured in air flow at the heating rate 6 K min^{-1}, a – Fe_2O_3/TiO_2 gels without PEG_{600} admixture, b – Fe_2O_3/TiO_2 gel with PEG_{600} admixture

out PEG_{600} heated to 300°C for 1 h increased considerably in comparison to the samples heated at 120°C. The surface area and porosity of PEG_{600} containing sample increased after heating to 300°C even more in comparison to the sample without PEG_{600} (*cf.* the surface area values 350 and 246 m^2 g^{-1}, respectively). These results are in agreement with the concept that the thermal decomposition of organic compounds included in the titania gel during synthesis was accompanied by the increase of the surface area and porosity of the samples [22]. A decrease in surface area and porosity of the samples heated beyond 400°C, that was supposed from the ETA results, was confirmed experimentally (Table 1).

The pore size distributions of the titania gel samples without and with the PEG_{600} admixture heated at 120 and at 300°C are presented in Figs 2a, b and Figs 3a, b, respectively. Both types of the samples possessed porous structures with pore diameters under 6 nm and from 6 up to 80 nm. In the samples heated at 300°C (i.e. after the thermal degradation of the organic compounds took place) the volume of pores of practically all mentioned sizes increased; moreover it should be pointed out that the number of pores larger than 80 nm increased in the sample after heating to 300°C. This can be attributed to the fact that the thermal degradation of PEG_{600} macromolecules in the Fe_2O_3/TiO_2 gel matrix favored the formation of mesopores.

For the titania based samples heated at 500°C the surface area decreased, namely for the sample without PEG_{600} it decreased to 75.8 m^2 g^{-1} and for the sample with PEG_{600} to 42.7 m^2 g^{-1}. The pore volume of the respective samples decreased to 0.119 and 0.057 mL g^{-1} (Table 1). Hence, the microstructure of the titania gel that contained PEG_{600} was less thermally stable and its porosity collapsed on heating in this temperature range more rapidly than for the sample without PEG_{600}. This is agreement with our ETA results in Figs 1a and b that characterized the thermal behavior of the samples. The ETA data of the titania gel samples without PEG_{600} (curve 1) and with PEG_{600} (curve 2) are compared in Fig. 4. From the decrease of the radon release rate observed on heating of the samples (Fig. 4) it follows that the surface area and porosity decrease took place in two steps, namely in the temperature ranges 230–400 and 400–600°C. The ETA results complemented the direct measurements of the porosity and surface area (Table 1).

From the XRD patterns (Figs 5 and 6) it followed that both samples with and without PEG_{600} are amorphous when heated at 300°C for 1 h. The titania sam-

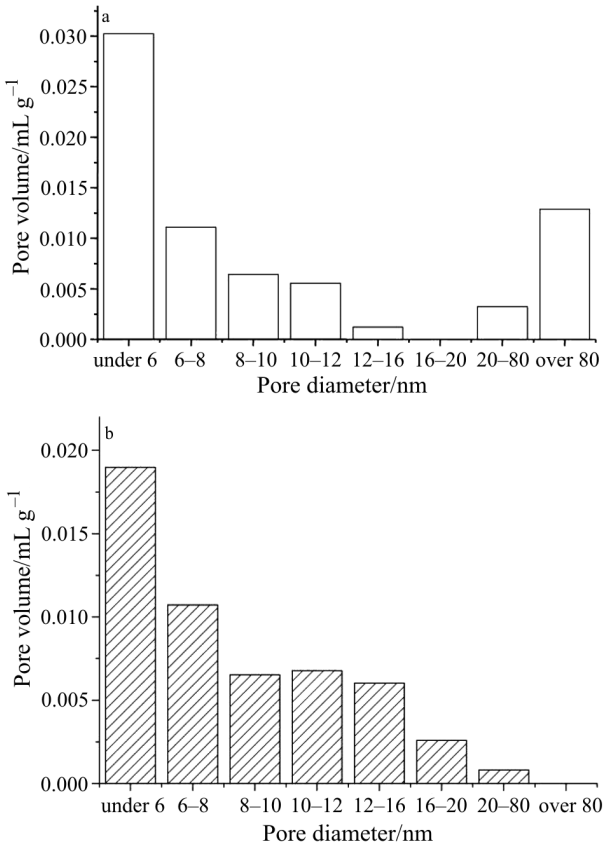

Fig. 2 Pore size distribution in the Fe_2O_3/TiO_2 gel samples heated at 120°C, a – sample without PEG_{600} admixture, b – sample with PEG_{600} admixture

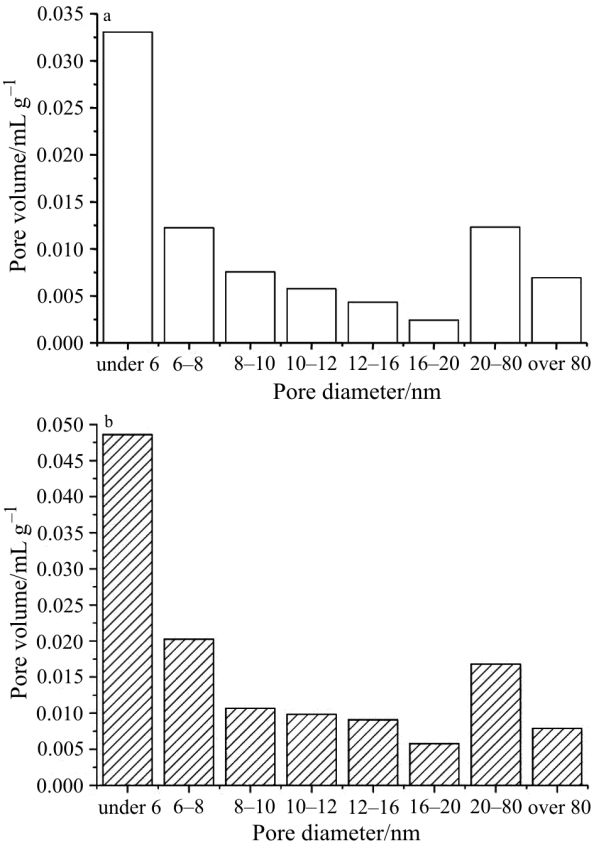

Fig. 3 Pore size distribution in Fe_2O_3/TiO_2 gel samples heated for 1 h at 300°C, a – sample without PEG_{600} admixture, b – sample with PEG_{600} admixture

ple without PEG_{600} remained amorphous up to 500°C while in the sample containing PEG_{600} the beginning of anatase formation was observed at this temperature. This is probably due to the fact that during the organic compounds oxidation the increase of local temperature enhanced the crystallization of nanocrystalline anatase. After heating to 600°C both titania samples possessed anatase structure. The crystallite size calculated by Scherrer equation [20] was 8.0 nm for the gel without PEG_{600} and 9.1 nm for the gel with PEG_{600} addition. So the difference in the crystallite size is small.

The ETA results were evaluated by a mathematical model recently developed [23]. The modeling background is briefly described in the Appendix of this paper. From Figs 7a and b it followed that a good agreement was obtained between the results of mathematical modeling the corresponding experimental ETA data. In the temperature range 50–250°C the increase of radon release rate was described by model curves 1, whereas in the range 250–600°C the decrease of the structure irregularities that served as radon diffusion paths, was modeled by curves 2.

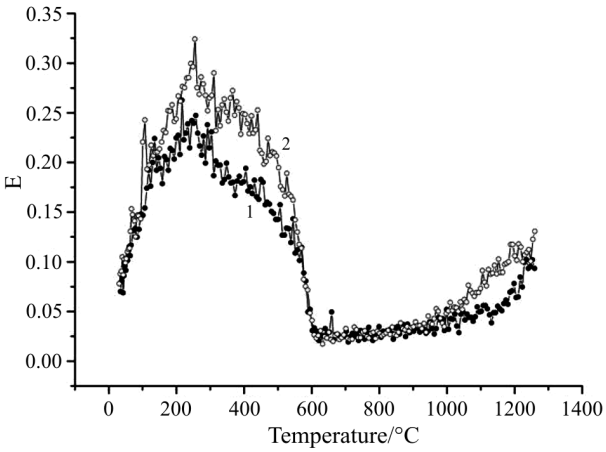

Fig. 4 Comparison of the ETA results of Fe_2O_3/TiO_2 gels without PEG_{600} admixture (curve 1) and with PEG_{600} admixture (curve 2)

In its turn, the thermal behavior of crystalline titania, characterized by ETA on heating from 600 to 1250°C, was described by the model curves 3 (Eqs (1) and (2) of the Appendix). The model functions $\Psi(T)$ that describe the decrease of surface area

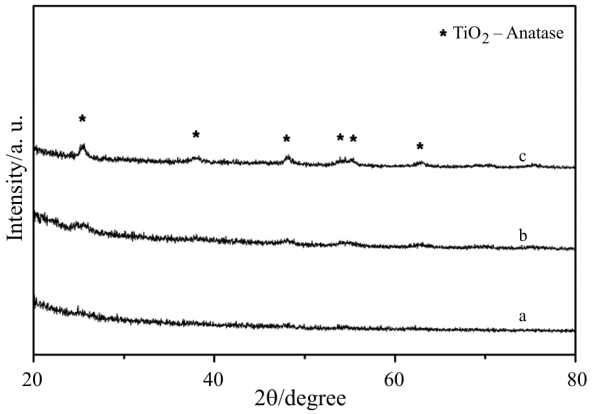

Fig. 5 XRD patterns of Fe_2O_3/TiO_2 samples without PEG_{600} admixture heated for 1 h at a – 300°C, b – 500°C and c – 600°C

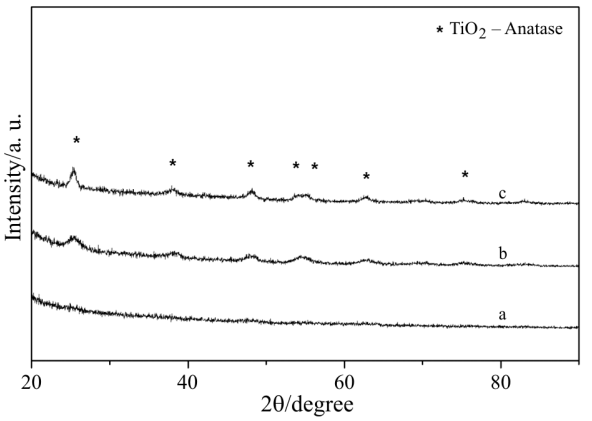

Fig. 6 XRD pattern of the Fe_2O_3/TiO_2 samples with PEG_{600} admixture heated 1 h at a – 300°C, b – 500°C and c – 600°C

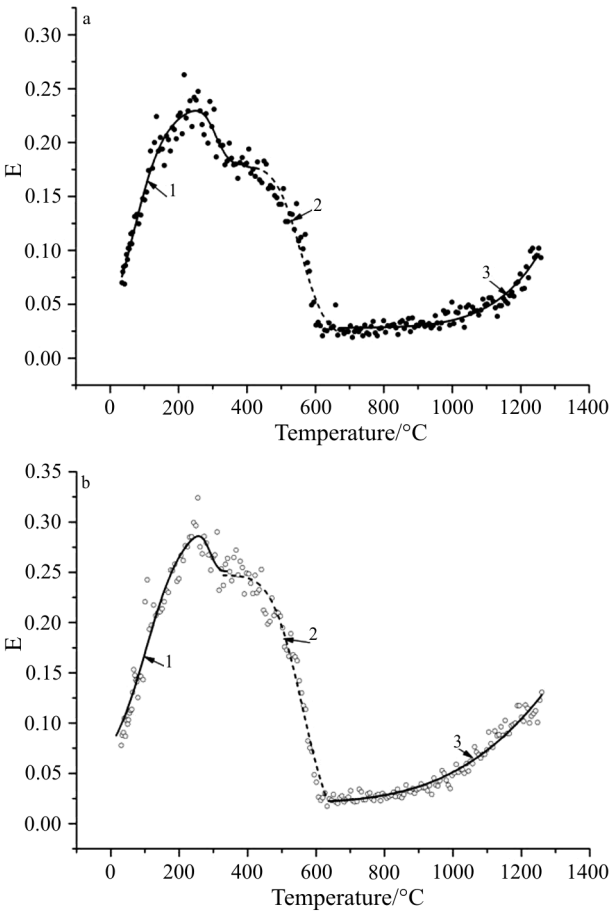

Fig. 7 Comparison of the experimental ETA results (points) with the corresponding results of modeling (curves 1, 2, 3 – lines) for the Fe_2O_3/TiO_2 gels, a – Fe_2O_3/TiO_2 gel without PEG_{600} admixture, b – Fe_2O_3/TiO_2 gel with PEG_{600} admixture

and open porosity were calculated by using Eq. (3) of the Appendix.

The results of modeling, namely the functions of $\Psi(T)$ and $d\Psi/dT$, that characterize differences in the microstructure changes during in situ heating of the titania samples are presented in Fig. 8. The decrease of the number of radon diffusion paths took place in the temperature range 230–400°C and monitored the microstructure changes of the intermediate products of the formation of the mesoporous titania samples. It should be mentioned that for the titania sample without PEG_{600} the maximum rate of the decrease was by 20°C higher than that for the titania sample with PEG_{600} (curve 1' and curve 2', respectively, in Fig. 8). From the comparison of curves 1 and 2 in Fig. 8 it is obvious that on heating above 400°C a more significant decrease of surface and open porosity took place for the sample that contained PEG_{600}. This is in agreement with the surface area and porosity data presented in Table 1.

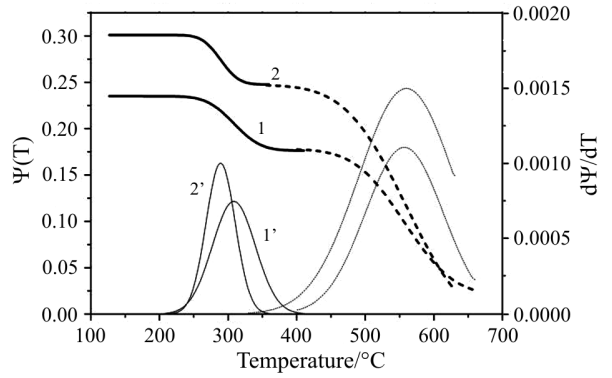

Fig. 8 Temperature dependences of model functions $\Psi(T)$ (curves 1 and 2) and $d\Psi/dT$ (curves 1' and 2') that describe microstructure annealing on heating of Fe_2O_3/TiO_2 gel samples: curves 1 and 1' correspond the gels without PEG_{600} admixture, curves 2 and 2' correspond the gels with PEG_{600} admixture

Conclusions

It was demonstrated that the emanation thermal analysis (ETA) brought about an additional information to that obtained by TG, DTA, EGA, XRD, surface area and porosity measurements. The thermal behavior the titania based mesoporous gels elucidated from the results of various methods made it possible to determine optimized conditions for the preparation of the Fe-doped titania based photocatalytic materials. The mathematical model applied in this study can be recommended for the evaluation of the ETA results obtained in our previous studies [24, 25].

Appendix

Background of the modeling of ETA results

In modeling the temperature dependences of radon release from solids it was assumed that the radon release from labelled samples is controlled by several mechanisms, namely: (*i*) release due to the recoil energy of radon atoms, (*ii*) diffusion in open pores, intergranular space or interface boundaries, respectively and (*iii*) radon diffusion in the matrix of solids. The expression for the measured radon release rate, E_{TOTAL} (also called emanating rate, E), can be written as

$$E_{TOTAL}(T)=E_0+E_D(T)\Psi(T) \quad (1)$$

where E_0 is emanating rate due to recoil and E_D is emanating rate due to diffusion. The E_D characterizes the radon permeability along structure irregularities serving as diffusion paths, and $\Psi(T)$ is the function characterizing the decrease (or increase) of the number of the radon diffusion paths, like, micropores, intergranular space, interface boundaries, etc. Following expression was used in for the temperature dependence of the emanating rate E_D, due to diffusion

$$E_D=(3/y)(\coth y-1/y) \quad (2)$$

where

$$y(T)=(S/M)\rho/(D/\lambda)^{1/2}$$

where S/M is the surface area of open pores, inter-granular space and of interfaces serving as radon diffusion paths, ρ is density of the sample, $(D/\lambda)^{1/2}$ is average radon diffusion length. D is the radon diffusion coefficient and λ =0.12 s^{-1} is radon decay constant; $D=D_0\exp(-Q/RT)$, where D_0 is the factor depending on the number of diffusion paths and their availability for radon atoms migration, Q is activation energy of radon migration involving both the activation energy of the escape of radon atoms from the traps in the solid and that of the migration along diffusion paths in the solid.

In the case that the number of radon diffusion paths and/or surface area decreases on heating, the structural function $\Psi(T)$ has descending character. Following expression [23] was used for the $\Psi(T)$ function

$$\Psi(T)=0.5\left[1+erf\frac{1-\frac{T_m}{T}}{\frac{\Delta T\sqrt{2}}{T}}\right] \quad (3)$$

where *erf* is the sign for the integral Gauss function, T_m is the temperature of maximal rate of the annealing of the defects which serve as radon diffusion paths, ΔT is the temperature interval of the respective solid-state process.

Acknowledgments

This work was supported by the Grant Agency of the Czech Republic (Project No. 104/04/0467. The financial support received for the bilateral science and technology cooperation between Greece and Czech Republic by Ministry of Education of the Czech Republic (Project ME 683) and by Ministry of Development of Greece is highly appreciated. Thanks are due to Dr. I. M. Bountseva, Moscow State University, for modeling the ETA results.

References

1 A. Fujishima, T. N. Rao and D. A. Tryk, J. Photochem. Photobiol., C1 (2000) 1.
2 M. R. Hoffman, S. T. Martin, W. Choi and D. W. Bahneman, Chem. Rev., 95 (1995) 69.
3 A. L. Linsebigler, G. Lu and G. T. Yates, J. Chem. Rev., 95 (1995) 735.
4 W. Choi, A. Termin and M. R. Hoffman, J. Phys. Chem., 89 (1994) 13669.
5 J. Nettleton-Hammond and M. A. Malati, React. Kinet. Catal. Lett., 70 (2000) 325.
6 C. C. Trapalis, P. Keivanidis, G. Kordas, M. Zaharescu, M. Crisan, A. Szatvanyi and A. Gartner, Thin Solid Films, 433 (2003) 186.
7 R. S. Sonawane, B. B. Kale and M. K. Dongare, Mater. Chem. Phys., (2004) in press.
8 E. Piera, I. M. Tejedor-Tejedor, M. E. Zorn and M. A. Anderson, Appl. Catal., B: Environmental, 46 (2003) 671.
9 M. Sokmen, F. Candan and Z. Sumer, J. Photochem. Photobiol., A: Chemistry, 143 (2001) 241.
10 J. Yu, X. Zhao, Q. Zhao and G. Wang, Mater. Chem. Phys., 68 (2001) 253.
11 X. Liu, J. Yang, L. Wang, X. Yang, L. Lu and X. Wang, Mater. Sci. Eng. A, 289 (2000) 241.
12 G. Xiong, X. Wamg, L. Lu, X. Yang and Z. Xu, J. Solid State Chem., 141 (1998) 70.
13 K. Kato and K. Niihara, Thin Solid Films, 298 (1997) 76.
14 K. Kato, A. Tsuge and K. Niihara, J. Am. Ceram. Soc., 79 (1996) 1483.
15 S. Musik, M. Gotic, M. Iivanda, S. Popovic, A. Turcovic, R. Trojko, A. Sekulic and K Furic, Mater. Sci. Eng., B, 47 (1997) 33.
16 V. Balek and J. Toelgyessy, Emanation Thermal Analysis and other Radiometric Emanation Methods, in G. Svehla (Ed.) Wilson and Wilson's Comprehensive Analytical Chemistry, Part XII.C, Elsevier Sci. Publ., 1984, pp. 43–71.

17 V. Balek, J. Šubrt, T. Mitsuhashi, I. N. Beckman and K. Györyova, J. Therm. Anal. Cal., 67 (2002) 15.
18 V. Balek, E. Klosova, N. Sumi, T. Mitsuhashi, H. Haneda and J. Šubrt, Thin Solid Films, 394 (2001) 40.
19 J. F. Ziegler and J. P. Biersack, The stopping and range of ions in solids, Pergamon Press, New York 1985.
20 D. K. Smith, in: D. L. Bish and J. E. Post (Eds), Modern Powder Diffraction, in: Reviews in Mineralogy, Vol. 20, Mineralogical Society of America, Washington, DC 1989, p. 183.
21 J. Bujdak, E. Hackkett and E. P. Gianellis, Chem. Mater., 12 (2000) 2168.
22 S. Ito, S. Inoue, H. Kawada, H. Hara, M. Iwasaki and H. Tada, J. Colloid Interface Sci., 216 (1999) 59.
23 I. N. Beckman and V. Balek, J. Therm. Anal. Cal., 67 (2002) 49.
24 V. Balek, Z. Malek, J. Šubrt, M. Guglielmi, P. Innozenzi, V. Rigato and G. Della Mea, J. Therm. Anal. Cal., 76 (2004) 43.
25 F. Kovanda, V. Balek, V. Dornicak, P. Martinec, M. Maslan, L. Bilkova, D. Kolousek and I. M. Bountseva, J. Therm. Anal. Cal., 71 (2003) 727.